Oxytocin regulates body composition

Li Sun[a,b], Daria Lizneva[a,b], Yaoting Ji[a,b,c], Graziana Colaianni[d], Elina Hadelia[a,b], Anisa Gumerova[a,b], Kseniia Ievleva[a,b], Tan-Chun Kuo[a,b], Funda Korkmaz[a,b], Vitaly Ryu[a,b], Alina Rahimova[a,b], Sakshi Gera[a,b], Charit Taneja[a,b], Ayesha Khan[a,b], Naseer Ahmad[a,b], Roberto Tamma[d], Zhuan Bian[e], Alberta Zallone[d], Se-Min Kim[a,b], Maria I. New[f,1], Jameel Iqbal[a,b], Tony Yuen[a,b,2], and Mone Zaidi[a,b,1,2]

[a]The Mount Sinai Bone Program, Icahn School of Medicine at Mount Sinai, New York, NY 10029; [b]Department of Medicine, Icahn School of Medicine at Mount Sinai, New York, NY 10029; [c]Department of Oral Biology, School of Stomatology, Wuhan University, 430076 Wuhan, China; [d]Department of Basic Medical Science, Neurosciences, and Sensory Organs, University of Bari Aldo Moro Medical School, 70126 Bari, Italy; [e]Department of Endodontics, School of Stomatology, Wuhan University, 430076 Wuhan, China; and [f]Department of Pediatrics, Icahn School of Medicine at Mount Sinai, New York, NY 10029

Contributed by Maria I. New, October 28, 2019 (sent for review August 13, 2019; reviewed by Xu Cao, Christopher Huang, and Yi-Ping Li)

The primitive neurohypophyseal nonapeptide oxytocin (OXT) has established functions in parturition, lactation, appetite, and social behavior. We have shown that OXT has direct actions on the mammalian skeleton, stimulating bone formation by osteoblasts and modulating the genesis and function of bone-resorbing osteoclasts. We deleted OXT receptors (OXTRs) selectively in osteoblasts and osteoclasts using *Col2.3Cre* and *Acp5Cre* mice, respectively. Both male and female *Col2.3Cre*$^{+}$:*Oxtr*$^{fl/fl}$ mice recapitulate the low-bone mass phenotype of *Oxtr*$^{+/-}$ mice, suggesting that OXT has a prominent osteoblastic action in vivo. Furthermore, abolishment of the anabolic effect of estrogen in *Col2.3Cre*$^{+}$:*Oxtr*$^{fl/fl}$ mice suggests that osteoblastic OXTRs are necessary for estrogen action. In addition, the high bone mass in *Acp5Cre*$^{+}$:*Oxtr*$^{fl/fl}$ mice indicates a prominent action of OXT in stimulating osteoclastogenesis. In contrast, we found that in pregnant and lactating *Col2.3Cre*$^{+}$:*Oxtr*$^{fl/fl}$ mice, elevated OXT inhibits bone resorption and rescues the bone loss otherwise noted during pregnancy and lactation. However, OXT does not contribute to ovariectomy-induced bone loss. Finally, we show that OXT acts directly on OXTRs on adipocytes to suppress the white-to-beige transition gene program. Despite this direct antibeiging action, injected OXT reduces total body fat, likely through an action on OXT-ergic neurons. Consistent with an antiobesity action of OXT, *Oxt*$^{-/-}$ and *Oxtr*$^{-/-}$ mice display increased total body fat. Overall, the actions of OXT on bone mass and body composition provide the framework for future therapies for osteoporosis and obesity.

pituitary hormone | conditional knockout | bone phenotype | adipose tissue

Oxytocin (OXT) exerts peripheral actions during parturition and milk ejection, and central actions to regulate appetite and social behavior in mammals (1, 2). We have previously shown that in mice, OXT is also a potent regulator of bone mass through its direct action on OXT receptors (OXTRs) identified on both osteoblasts and osteoclasts (3–5). We find that the global deletion of the *Oxt* or *Oxtr* genes results in profound age-associated osteopenia (5). In in vitro assays, OXT stimulates osteoblasts toward a more differentiated, mineralizing phenotype while displaying a dual action on osteoclasts (5). Namely, OXT enhances osteoclast formation from hematopoietic stem cell precursors but inhibits the activity of mature osteoclasts by triggering the production of nitric oxide (5), a naturally occurring inhibitor of bone resorption (6). It remains unclear, particularly in the light of a reduced bone mass in *Oxt*$^{-/-}$ and *Oxtr*$^{-/-}$ mice, as to which if any osteoclastic actions predominate in the physiological context. These studies are important because in humans and rodents, plasma OXT levels rise during late pregnancy and lactation, a period coinciding with demineralization of the maternal skeleton in favor of the intergenerational transfer of calcium ions for fetal skeletal morphogenesis and, postnatally, for lactation. The maternal skeleton is then repaired normally without a net loss of bone, with excessive bone loss leading to the osteoporosis of pregnancy and lactation. In this study, using transgenic mice expressing Cre recombinase driven by the 2.3-kb *Col1a1* or *Acp5* promoter, we examined the effect of deleting the *Oxtr*s on the osteoblast and osteoclast lineages, respectively.

OXT is also known to affect body weight by inhibiting feeding through a central action on hypothalamic paraventricular neurons. Chronic central OXT infusion in high-fat diet–induced obese rats thus results in decreased body weight, increased adipose tissue lipolysis, increased fatty acid β-oxidation, and reduced glucose intolerance and insulin resistance (7). Hyperphagic obese patients harboring an *SIM1* gene mutation or with Prader–Willi syndrome display reduced numbers and sizes of OXT-ergic neurons in paraventricular nuclei (8, 9). While these findings suggest that the prominent effects of OXT on body composition are mediated centrally through satiety, there is limited evidence of peripheral action. The late-onset obesity in *Oxtr*$^{-/-}$ mice appears to be independent of daily intake of chow (10); however, both s.c. and i.p. OXT injections modify food intake (11, 12), suggesting that peripheral OXT could cross the blood-brain barrier. Here we describe a hitherto unknown direct peripheral action of OXT on adipocyte OXTRs—a cell-autonomous antibeiging action to conserve energy—that may be compensatory to the centrally mediated reduction in body fat.

Results

We have shown previously that the global deletion of *Oxt* or *Oxtr* results in a low-bone mass phenotype that worsens with age (5).

Significance

We show here that oxytocin (OXT), a hormone derived from the posterior pituitary gland, stimulates the synthesis of new bone while preventing bone loss during pregnancy and lactation, when fetal demands for calcium and plasma OXT levels are high. In addition, OXT reduces body fat, but as a compensatory mechanism, prevents white-to-beige transition, enabling energy conservation. The study provides the premise for a primary role for OXT in the physiologic regulation of bone mass and body fat, lending itself and its receptor as targets for future therapies to combat osteoporosis and obesity, diseases that affect millions of men and women worldwide.

Author contributions: L.S., D.L., A.Z., M.I.N., and M.Z. designed research; L.S., D.L., Y.J., G.C., E.H., A.G., K.I., T.-C.K., F.K., V.R., S.G., C.T., A.K., R.T., and T.Y. performed research; L.S., D.L., Y.J., G.C., E.H., A.R., N.A., R.T., Z.B., A.Z., S.-M.K., J.I., T.Y., and M.Z. analyzed data; and M.I.N., T.Y., and M.Z. wrote the paper.

Reviewers: X.C., Johns Hopkins School of Medicine; C.H., University of Cambridge; and Y.-P.L., University of Alabama at Birmingham.

The authors declare no competing interest.

Data deposition: The complete dataset for this article has been deposited in the Open Science Framework, https://osf.io/ws98e/?view_only=8d17370ec6f74d88a909ed02f1c12321.

[1]To whom correspondence may be addressed. Email: maria.new@mssm.edu or mone.zaidi@mssm.edu.

[2]T.Y. and M.Z. contributed equally to this work.

First published December 16, 2019.

Here, using micro-computed tomography (μCT) imaging, we document that this phenotype, shown as reductions in bone mineral density (BMD), fractional bone volume (BV/TV), and connectivity density (Conn.D), arises from a notable decrease in the number (Tb.N) rather than in the thickness (Tb.Th) of individual trabeculae in 10-mo-old male and female mice (Fig. 1 *A* and *B*). This is consistent with a full-thickness perforation and loss of trabecular structures, as opposed to their thinning (13). Haploinsufficient male $Oxt^{+/-}$ littermates also showed similarly significant differences except in Conn.D, suggesting a gene dosage effect (Fig. 1*A*).

We further explored whether OXT plays a role in the bone loss that follows ovariectomy, which our previous studies have attributed partly to elevated levels of follicle-stimulating hormone (FSH)

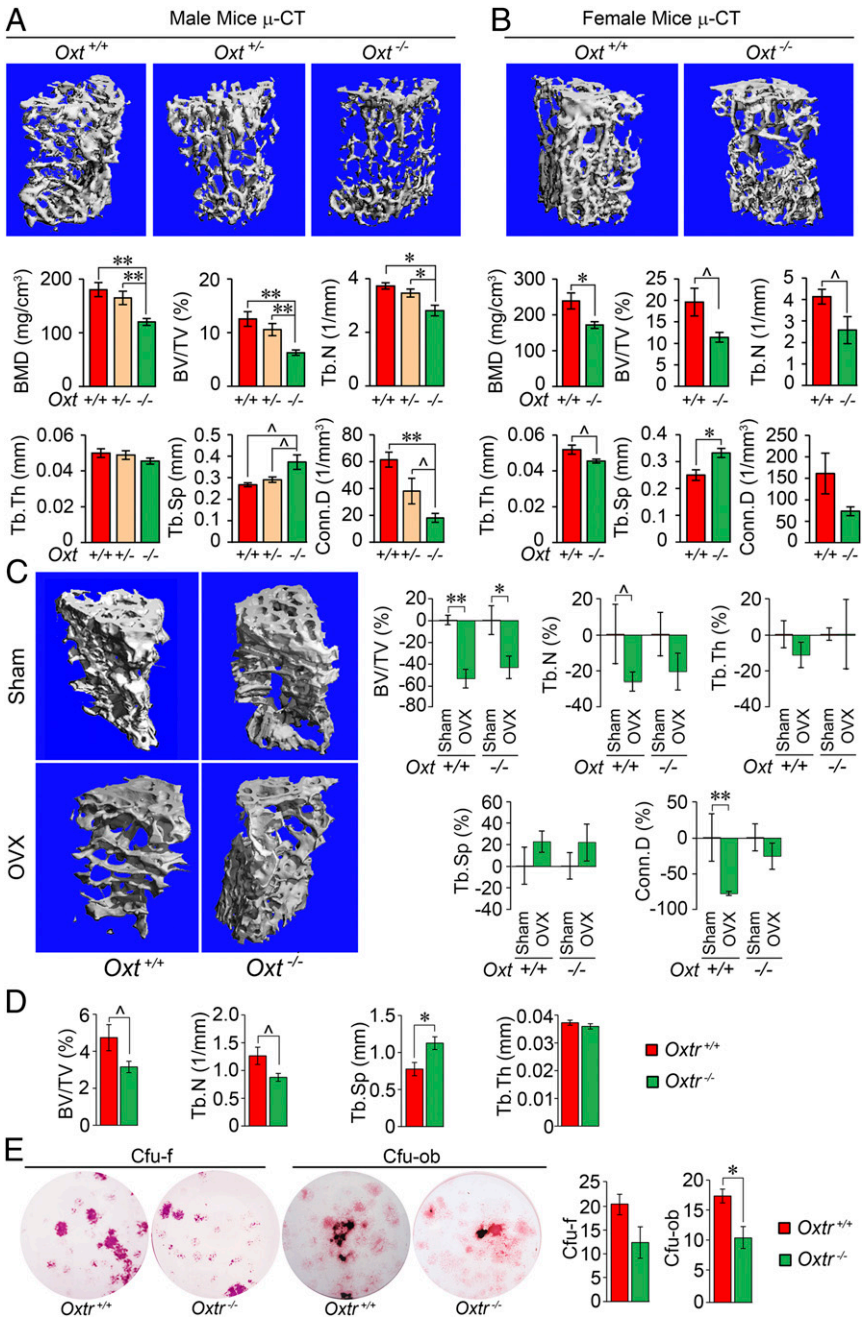

Fig. 1. OXT deficiency reduces bone mass but does not affect ovariectomy-induced bone loss. Representative μCT images and trabecular bone microstructural parameters—BMD, BV/TV, Tb.N, Tb.Th, trabecular spacing (Tb.Sp), and Conn.D—of 10-mo-old male (*A*) and female (*B*) wild-type (+/+), heterozygotes (+/–), or homozygotes (–/–) for the oxytocin gene, *Oxt* ($n = 4$ to 8 mice per group). (*C*) Representative μCT images and microstructural parameters (% control) showing the effect of ovariectomy (OVX) or sham operation (Sham; control) on 2-mo-old $Oxt^{+/+}$ and $Oxt^{-/-}$ mice ($n = 3$ to 9 per group). (*D*) μCT-based trabecular bone microstructural parameters in female wild-type and Oxtr-deficient ($Oxtr^{-/-}$) mice ($n = 3$ to 4 *per* group). (*E*) Representative cultures and quantitation of CFU-F stained for alkaline phosphatase and CFU-OB labeled with von Kossa stain. The colonies formed when bone marrow stromal cells isolated from $Oxtr^{+/+}$ or $Oxtr^{-/-}$ mice were allowed to grow in differentiation media (β-glycerol phosphate, ascorbic acid, and dexamethasone) for 7 and 21 d, respectively. Colonies per well were counted in triplicate. Data are expressed as mean ± SEM; comparisons with control mice, or as shown; $*P < 0.05$, $**P < 0.01$, or showing a trend $\wedge 0.05 < P < 0.1$, 2-tailed Student's *t* test or one-way ANOVA with Holm–Sidak correction.

in addition to the loss of estrogen (14, 15). For this, we ovariectomized or sham-operated $Oxt^{-/-}$ mice and wild-type littermates. At 4 wk after either procedure, the postovariectomy decline in BV/TV largely persisted (Fig. 1*C*), confirming that, in contrast to FSH, OT does not to play a major role in hypogonadal bone loss.

We evaluated whether the 3D microstructural phenotype of $Oxt^{-/-}$ mouse bones is recapitulated in $Oxtr^{-/-}$ mice. μCT-based measures of BV/TV and Tb.N were reduced in $Oxtr^{-/-}$ mice compared with their wild-type littermates, with no change in Tb.Th (Fig. 1*D*). This was accompanied at the cellular level by a reduction in the formation of colony-forming unit osteoblastoids (CFU-OB), which signifies stromal cell maturation into a mineralizing phenotype (Fig. 1*E*).

To validate the osteoblasts as a key OXT target, we conditionally deleted OXTRs selectively in the cells of the osteoblastic lineage using a transgenic mouse line expressing Cre under control of the 2.3-kb *Col1a1* promoter. $Col2.3Cre^{+}$:$Oxtr^{fl/fl}$ mice showed a robust reduction in BMD and BV/TV compared with a pooled control group consisting of Cre recombinase-negative $Col2.3Cre^{-}$:$Oxtr^{fl/+}$ and $Col2.3Cre^{-}$:$Oxtr^{fl/fl}$ mice (Fig. 2*A*). Interestingly, while Tb.N was reduced in the global $Oxtr^{-/-}$ mice (Fig. 1*A*), testifying to increased bone resorption and trabecular perforation, the reduction of Tb.Th was more consistent with reduced bone formation in osteoblast-specific OXTR mutants. The latter was confirmed histomorphometrically through calcein-xylelol orange labeling showing significant reductions in parameters of bone formation, namely mineral apposition rate (MAR) and bone formation rate (BFR) (Fig. 2*B*). Furthermore, there appeared to be a gene-dose effect. The respective parameters in $Col2.3Cre^{+}$:$Oxtr^{fl/+}$ haploinsufficient mice were between those of the control group and the $Col2.3Cre^{+}$:$Oxtr^{fl/fl}$ mice (Fig. 2*A*).

We determined whether the action of OXT on osteoblast OXTRs underpinned the anabolic action of estrogen (16), as predicted from preliminary observations (17). For this, we treated $Col2.3Cre^{+}$:$Oxtr^{fl/fl}$ mice and control ($Col2.3Cre^{-}$:$Oxtr^{fl/fl}$) littermates biweekly with 17β-estradiol (50 μg/kg) for 4 wk, with weekly areal BMD measurements by dual energy X-ray absorptiometry (DXA). The 17β-estradiol administration to control mice with intact osteoblastic OXTRs resulted in increased BMD at all sites (lumbar spine, femur, and tibia) over the 4-wk time course (Fig. 2*C*). This response was completely blunted in $Col2.3Cre^{+}$:$Oxtr^{fl/fl}$ mice to the no estrogen treatment level, with statistical significance achieved at the spine at 4 wk. The results of this extended study confirm our hypothesis that osteoblast OXTRs are required for the anabolic action of estrogen, although OXT does not appear to have a major role in mediating the bone loss due to estrogen withdrawal postovariectomy (Fig. 1*C*).

Previous collaborative studies with the Alberta Zallone group have documented the in vitro effects of OXT on both osteoclast formation and bone resorption by mature cells (3, 5). Whereas OXT stimulates osteoclast formation, it inhibits the resorptive activity of mature cells (5). We hypothesized that although the former action would enhance resorption, the latter action would prevent it. Thus, to examine the role of OXT in regulating osteoclasts in vivo, we created a mouse in which the *Oxtr* was deleted specifically in osteoclasts expressing *Acp5*, the gene encoding type 5A tartrate-resistant acid phosphatase (TRAP); this yielded $Acp5Cre^{-}$:$Oxtr^{fl/fl}$ (control) and $Acp5Cre^{+}$:$Oxtr^{fl/fl}$ mice. While initial observations had suggested the absence of a bone phenotype on areal BMD measurements by DXA in 16-wk-old $Acp5Cre^{+}$:$Oxtr^{fl/fl}$ mice, we find here that 6-mo-old mice, particularly females, showed trends or significant increases in BMD, BV/TV, Conn.D, Tb.N., and Tb.Th (Fig. 2*D*). These findings suggest that the high bone mass phenotype, which appears to be due mainly to a predominant reduction in osteoclastogenesis (vs. osteoclastic resorption), emerges with age in OXTR-deficient mice, causing an increase in bone mass in aging $Acp5Cre^{+}$:$Oxtr^{fl/fl}$ mice. However, in global *Oxtr* knockout mice, this protection through the inhibition of osteoclastogenesis cannot compensate for osteoblastic dysfunction, resulting in an overall reduction in bone mass. It is unlikely that Oxt levels are altered due to hormone resistance, as the OXTR is deleted only in osteoblasts or osteoclasts.

We attempted to examine the osteoclastic action of OXT under a period of physiological calcium stress, notably pregnancy and lactation, when bone remodeling is elevated and circulating OXT levels are high (18). While various hormonal mechanisms, including falling estrogen and high parathyroid hormone-related protein levels, have been proposed to underpin maternal bone resorption during pregnancy and lactation (18–21), high OXT may play a role in enhancing osteoclastogenesis to increase mineral dissolution from bone to favor fetal skeletal mineralization and milk production, respectively. To dissect the potential role of osteoclastic OXTRs, we studied bone mass across pregnancy and lactation in $Col2.3Cre^{+}$:$Oxtr^{fl/fl}$ mice lacking OXTRs in osteoblasts. Any phenotype during pregnancy and/or lactation in these mice would result from the action of high circulating OXT on intact osteoclastic OXTRs (in addition to absent osteoblastic OXTRs per se). We found that $Col2.3Cre^{+}$:$Oxtr^{fl/fl}$ mice display higher bone mass than wild-type mice during and after pregnancy, with a statistically significant difference at 14 d postlactation (Fig. 2*E*). This higher bone mass could not possibly be due to the absence of OXTRs in $Col2.3Cre^{+}$:$Oxtr^{fl/fl}$ osteoblasts, as OXT stimulates rather than inhibits bone formation (5). Thus, we posit that high circulating OXT puts a "brake" on resorption by mature osteoclasts while enabling mineral dissolution through enhanced osteoclastogenesis, a balance protective against excessive pregnancy- and lactation-induced bone loss.

We have previously shown that pituitary hormones, such as FSH, can regulate both bone mass and body fat (22). We studied the action of OXT on body fat in $Oxt^{-/-}$ and $Oxtr^{-/-}$ mice using DXA. Both male and female mice lacking OXT progressively gained body fat, measured both as total fat mass and as a percentage of total body weight, up to 11 mo (Fig. 3*A*). Likewise, body fat in both male and female $Oxtr^{-/-}$ mice was higher compared with wild-type littermates (Fig. 3*B*). There was no discernable difference in lean mass or total body weight in all 4 genotypes (Fig. 3 *A* and *B*). These data are concordant with a previous report showing a gain of body fat in $Oxtr^{-/-}$ mice, which, importantly, was independent of daily chow intake (10). Furthermore, we did not observe a difference in fat or lean mass in mice lacking OXTRs in osteoblasts, namely in $Col2.3Cre^{+}$:$Oxtr^{fl/fl}$ mice compared with control $Col2.3Cre^{-}$:$Oxtr^{fl/fl}$ mice (Fig. 3*C*). This finding suggests that OXT-mediated signals from the osteoblast did not modulate the proadiposity effects of OXTR deletion. In complementary gain-of-function experiments in 12-wk-old wild-type male, there was a reduction in percent fat mass as early as 1 wk but with no change in total body weight or percent lean mass (Fig. 3*D*). Documented reductions in food intake (11, 12), mediated centrally via central OXT-ergic neurons (Fig. 4), could potentially explain the reduction in body fat.

We were thus prompted to explore whether OXT displayed as-yet uncharacterized cell-autonomous peripheral actions on adipocytes. Fig. 4*A* shows a comprehensive quantitative PCR (qPCR) dataset for the expression of OXTRs in tissues from wild-type mice. We found that white adipose tissue (WAT) and brown adipose tissue (BAT) express OXTRs in both male and female mice, with some important relative differences. First, *Oxtr* expression in WAT from subcutaneous and visceral compartments was considerably higher in female mice compared with male mice. Second, *Oxtr* levels in subcutaneous and visceral WAT exceeded those in ovarian and uterine tissue, the latter being a primary target tissue for OXT. Finally, *Oxtr* expression in BAT was relatively low in both male and female mice.

The qPCR data were broadly consistent with the results of Western blot analysis using an anti-OXTR antibody (Abcam; ab181077), which showed protein expression in subcutaneous,

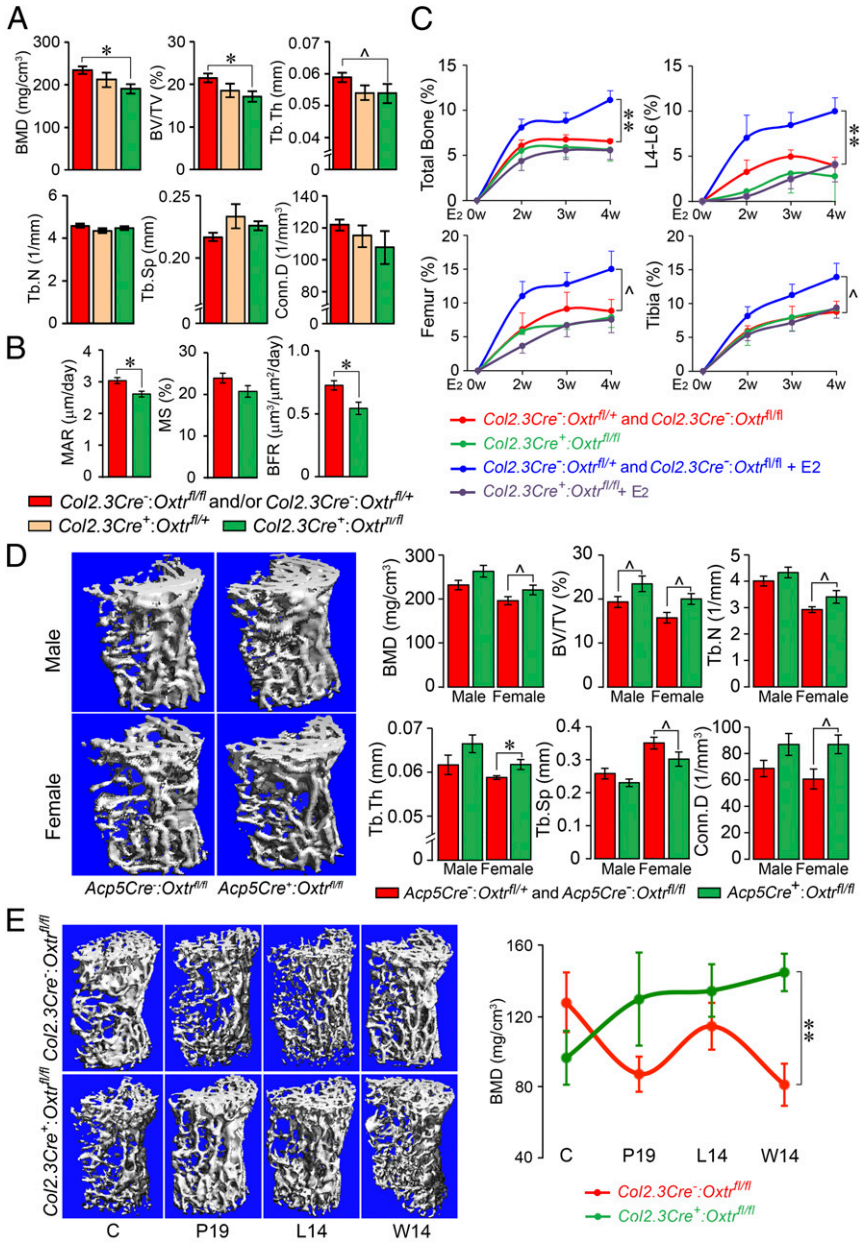

Fig. 2. Cell-selective mutants for the oxytocin receptor display bone mass phenotypes. (*A*) Trabecular bone microstructural parameters—BMD, BV/TV, Tb.Th, Tb.N, trabecular spacing (Tb.Sp), and Conn.D—of 4-mo-old male mice lacking or haploinsufficient in the *Oxtr* gene in osteoblasts (*Col2.3Cre*$^{+}$:*Oxtr*$^{fl/fl}$ or *Col2.3Cre*$^{+}$:*Oxtr*$^{fl/+}$ mice) or control littermates with the intact *Oxtr* gene (pooled, *Col2.3Cre*$^{-}$:*Oxtr*$^{fl/fl}$ and *Col2.3Cre*$^{-}$:*Oxtr*$^{fl/+}$ mice) ($n = 4$ to 9 mice per group). (*B*) Reduced bone formation parameters—MAR, mineralizing surface (MS), and BFR—in mature female *Col2.3Cre*$^{+}$:*Oxtr*$^{fl/fl}$ mice compared with control *Col2.3Cre*$^{-}$:*Oxtr*$^{fl/fl}$ mice ($n = 5$ mice per group). (*C*) Total bone, lumbar spine (L4 to L6), femoral, and tibial areal BMD showing the effect of 17β-estradiol (50 μg/kg) or vehicle injected biweekly over 4 wk into *Col2.3Cre*$^{+}$:*Oxtr*$^{fl/fl}$ or pooled control *Col2.3Cre*$^{-}$:*Oxtr*$^{fl/fl}$ and *Col2.3Cre*$^{-}$:*Oxtr*$^{fl/+}$ mice ($n = 4$ to 10 mice *per* group). (*D*) Representative μCT images of trabecular and microstructural parameters of 3-mo-old male and female mice lacking the *Oxtr* gene in osteoclasts (*Acp5Cre*$^{+}$:*Oxtr*$^{fl/fl}$ mice) or control littermates (pooled *Acp5Cre*$^{-}$:*Oxtr*$^{fl/fl}$ and *Acp5Cre*$^{-}$:*Oxtr*$^{fl/+}$ mice) ($n = 3$ to 12 mice *per* group). (*E*) Representative μCT images of trabecular bone and BMD at various times during pregnancy (day 19, P19), lactation (day 14, L14) and weaning (day 14, W14) ($n = 3$ to 6 mice *per* group). Data are expressed as mean ± SEM; comparisons with control mice, $^{*}P < 0.05$, $^{**}P < 0.01$, or showing a trend $^{\wedge}0.05 < P < 0.1$, 2-tailed Student's *t* test.

visceral, and perigonadal WAT and interscapular BAT in addition to the ovary, uterus, and liver in female mice (Fig. 4*B*). Immunohistochemistry analysis using the same antibody revealed specific OXTR labeling in subcutaneous and visceral WAT and BAT and in the adrenals and uterus (Fig. 4*C*). Immunofluorescence confirmed OXTR expression in various brain regions, including the nucleus tractus solitarius, lateral reticular nucleus, inferior olive nucleus, and raphe pallidus (Fig. 4*D*). We unequivocally confirmed OXTR expression in visceral and gonadal WAT and BAT by Sanger sequencing (partial cDNA sequence from coding nucleotide position 556 to the stop codon).

The high OXTR expression in WAT led us to study the effect of OXT on the expression of a panel of adipocyte genes. qPCR of RNA isolated from 3T3.L1 cells after a 14-d adipogenic induction and a 48-h incubation with OXT revealed profound reductions in the expression of key genes associated with white-to-beige transition ("beiging"), namely *Cox8b*, *Cebpb*, and *Cidea* (Fig. 4*E*). This suggests that OXT, despite decreasing body fat in intact

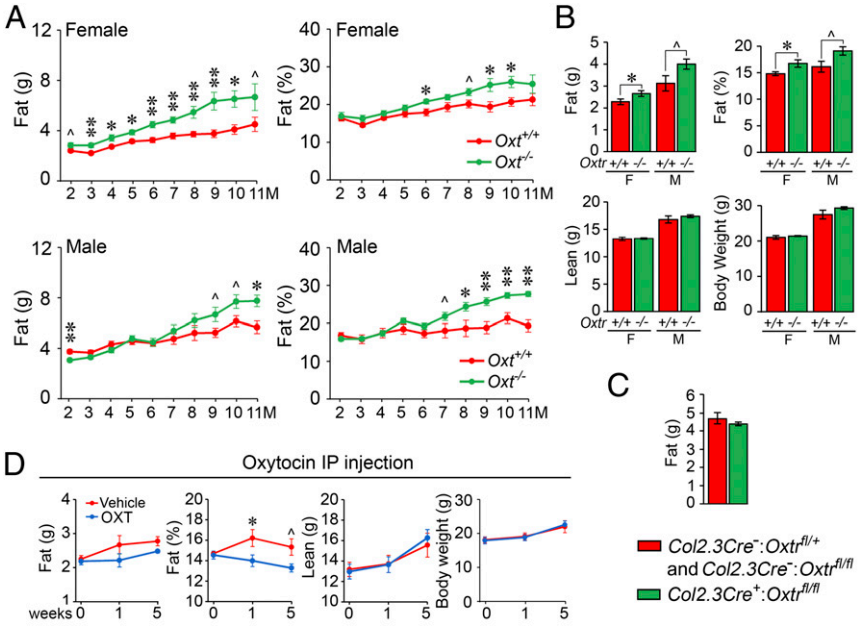

Fig. 3. Oxytocin signaling directly affects body fat. Incremental enhancements in body fat (% of total body weight) in male and/or female mice deficient in OXT ($Oxt^{-/-}$ mice) (*A*) or the OXT receptor ($Oxtr^{-/-}$ mice) (*B*) compared with their respective wild-type littermates ($Oxt^{+/+}$ or $Oxtr^{+/+}$ mice) measured by the GE Lunar Piximus ($n = 4$ to 7 mice per group). (*C*) No such difference was noted in mice lacking OXTRs specifically in osteoblasts, namely in $Col2.3Cre^{+}$:$Oxtr^{fl/fl}$ vs. control $Col2.3Cre^{-}$:$Oxtr^{fl/fl}$ and $Col2.3Cre^{-}$:$Oxtr^{fl/+}$ mice. This latter finding suggests that signals from the osteoblast did not modulate the proadiposity effects of OXTR deletion ($n = 4$ to 5 mice *per* group). (*D*) Effect of i.p. OXT injection on fat mass (g and %), lean mass (g), and total body weight (g) over 5 wk of treatment ($n = 6$ to 7 mice per group). Data are expressed as mean ± SEM; comparisons with control mice, $*P < 0.05$, $**P < 0.01$, or showing a trend $\hat{}0.05 < P < 0.1$, 2-tailed Student's *t* test.

mice, induces an antibeiging phenotype at the cellular level, likely as a compensatory mechanism to conserve energy. Furthermore, there were trends toward OXT-induced reductions in the expression of *Fabp4*, *Cox7a1*, and *Retn*, whereas no differences in *Irs1*, *Pparg*, *Adipoq*, *Cebpa*, and *Insr* expression were seen (Fig. 4*E*). Interestingly, expression of the steroidogenic gene *Hsd17b12* was elevated significantly. Furthermore, and of note, *Serpine1*, a gene that encodes plasminogen activator inhibitor 1 (PAI1), was increased by 5-fold in OXT-treated adipocytes compared with controls.

Discussion

The present study explored the actions of OXT beyond its traditionally recognized peripheral effects on parturition and lactation and central effects on appetite and social behavior (1, 2). We have found that OXT is a bone anabolic hormone that acts primarily to promote osteoblast maturation to a mineralizing phenotype and regulates both the genesis and function of bone resorbing osteoclasts (5). We posit that this set of biological actions, which may also require internalization of the OXTR (23), underscore the regulated intergenerational transfer of calcium ions during pregnancy and lactation in favor of fetal skeletal mineralization and milk production, respectively (24). Therefore, we have studied the mechanism of the skeletal action of OXT in depth using mice that lack OXTRs specifically in osteoblasts or osteoclasts.

Our finding that the low bone mass of $Col2.3Cre^{+}$:$Oxtr^{fl/fl}$ mice lacking osteoblastic OXTRs recapitulates the global $Oxtr^{-/-}$ phenotype attests to a dominant action of OXT on the osteoblast. Our (admittedly speculative) hypothesis is that the anabolic action of OXT could potentially underpin the rescue of the maternal skeleton postlactation when circulating OXT levels are high. We have previously shown in vitro that OXT stimulates the genesis of osteoclasts while inhibiting the resorptive activity of mature cells (5). This raises a second question as to which of the 2 opposing actions of OXT on the osteoclast—stimulation of osteoclastogenesis or inhibition of resorptive activity—contributes to the overall skeletal action of OXT in vivo. We show that $Acp5Cre^{+}$:$Oxtr^{fl/fl}$ mice exhibit high bone mass with age. This phenotype in OXTR-less osteoclasts can only be explained by a reduction of osteoclastogenesis. We also surmise that while OXT may enable the formation of new osteoclasts, it would prevent unrestricted resorption by ensuring a "brake" on their activity. Thus, when we examined osteoclastic actions of high OXT levels in pregnant $Col2.3Cre^{+}$:$Oxtr^{fl/fl}$ mice (lacking osteoblastic OXTRs), we found that bone resorption was prevented, resulting in a higher bone mass than seen in control pregnant mice. This suggests that under calcium stress, OXT can mobilize calcium but can also be used as a "brake" preventing excessive bone dissolution.

We also explored the interaction of OXT and estrogen, having shown previously that the action of pharmacologic doses of 17β-estradiol, used widely in clinical practice in postmenopausal women, was mediated via OXT (17). We have shown that estrogen stimulates the expression of both OXT and OXTRs in osteoblasts (3, 17, 23). Furthermore, in addition to our preliminary study (17), here we prove that the absence of OXTRs specifically in osteoblasts in $Col2.3Cre^{+}$:$Oxtr^{fl/fl}$ mice completely abolishes estrogen's anabolic action on the skeleton. This is in stark contrast to the nonrequirement of OXT for hypogonadal bone loss noted on ovariectomy, which persists in the absence of global OXTR signaling. Indeed, this is in line with our premise that high FSH and low estrogen jointly contribute to bone loss postovariectomy, and that this loss is rescued both after estrogen replacement and after the administration of an anti-FSH antibody (14, 15). Therefore, overall our dataset establishes OXT signaling as necessary for the anabolic action of estrogen on bone, while confirming an absent function for OXT in the bone loss of hypogonadism.

Over the past decade, we have provided evidence for a pituitary-bone axis through which pituitary hormones, including OXT, can bypass traditional targets and affect the skeleton directly (25, 26). This axis has been extended to encompass effects of pituitary

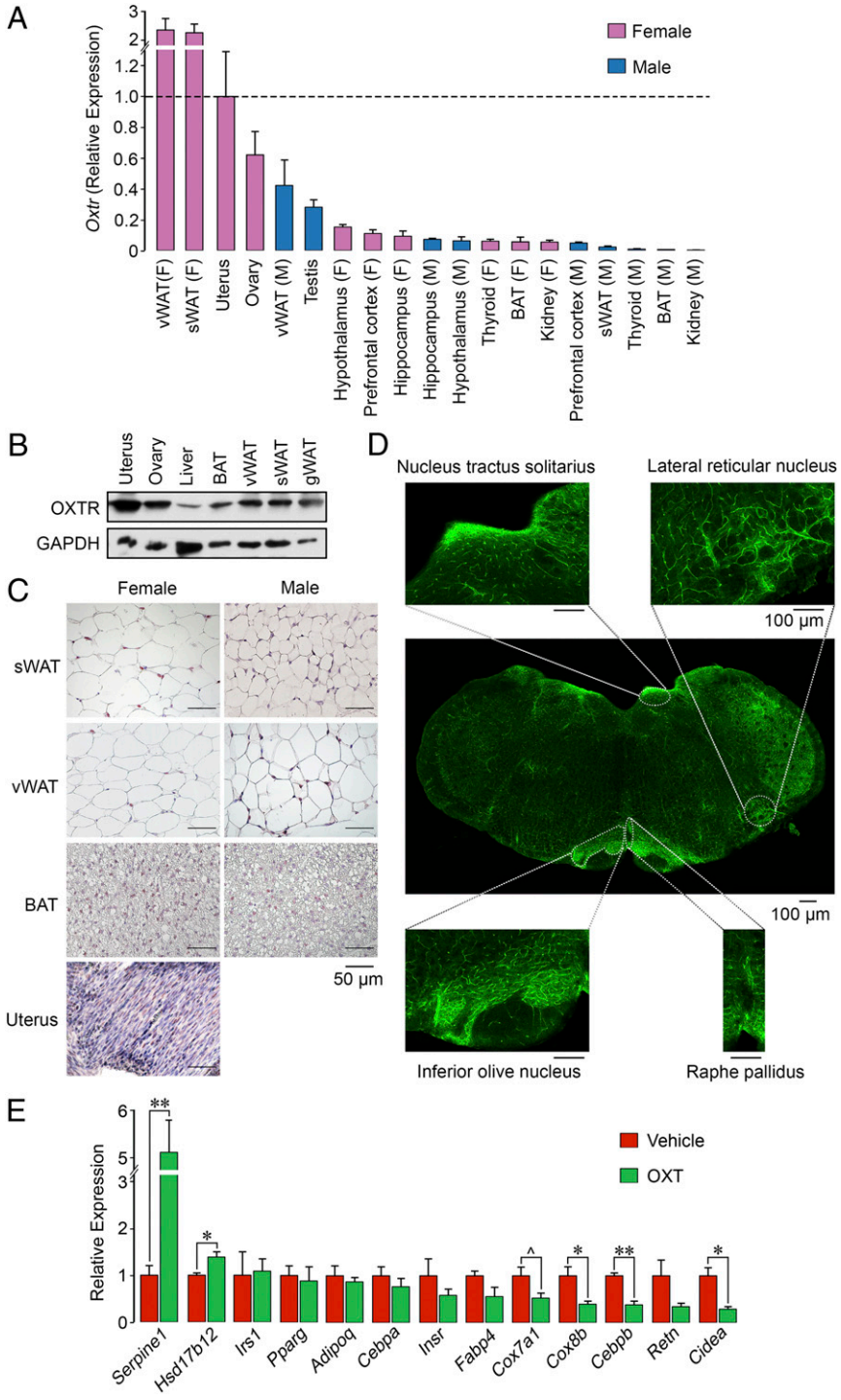

Fig. 4. Oxytocin acts on adipocyte oxytocin receptors to suppress beiging. (*A*) qPCR showing the expression of OXTR in mouse tissues of interest, including the uterus, ovary, testes, 3 brain regions, and visceral (v) and subcutaneous (s) WAT and BAT. (*B*) Western blot analysis using an anti-OXTR antibody (Abcam; ab181077) showed OXTR protein expression in female uterus, ovary, liver, BAT, and visceral, subcutaneous, and perigonadal WAT. Glyceraldehyde 3-phosphate dehydrogenase (GAPDH) served as a loading control. (*C*) Immunohistochemistry using the same anti-OXTR antibody confirming high expression levels in uterus, with a strong signal in subcutaneous and visceral WAT and limited expression in BAT. (Scale bar: 50 μm.) (*D*) Immunofluorescence images of OXTR expression in various brain regions, including the nucleus tractus solitarius, lateral reticular nucleus, inferior olive nucleus, and raphe pallidus. The whole brain section was composed from 12 images. (Scale bar: 100 μm.) (*E*) qPCR on RNA isolated from adipocytes derived from precursor 3T3.L1 cells following a 14-d incubation in differentiation medium and a 2-d incubation with OXT. There was a significant ($*P < 0.05$, $**P < 0.01$) reduction in or a trend toward reduced expression ($\hat{}0.05 < P < 0.1$) of certain genes involved in beiging, namely *Cox7a*, *Cox8b*, *Cebpb*, *Retn*, and *Cidea*. Certain genes involved in steroidogenesis and thrombosis, namely *Hsd17b12* and *Serpine1*, respectively, were up-regulated. The qPCR data were normalized to housekeeping genes *Actb* (*A*) *Gapdh* (*A* and *D*), *Rps11* (*A* and *D*), and *Tuba1a* (*A* and *D*). Three biological replicates with 3 technical replicates were used. Data are expressed as mean ± SEM; comparisons with vehicle treatment, 2-tailed Student's *t* test.

hormones on body composition, such as in the case of FSH, where reduced FSH signaling is associated with increased bone mass and reduced body fat (22, 27). We now extend the concept of a pituitary-metabolic circuit to include OXT. Anorexigenic actions of OXT, which lead to the induction of satiety following a central hypothalamic action, have been described previously (11, 28). Injection of OXT leads to reduced appetite and body weight in mice (7, 11, 12). Consistent with this, patients with hyperphagic obesity, such as those with Prader–Willi syndrome, display reduced numbers and size of OXTR-ergic neurons in paraventricular nuclei (8, 9). However, whether peripheral actions of OXT may in addition regulate body composition remains unclear. We found high levels of OXTR expression at both RNA and protein levels in WAT and lower levels in BAT. Furthermore, the application of OXT to adipocytes derived from 3T3.L1 precursors inhibits the beiging gene program. An antibeiging action in the face of loss of body fat due to centrally induced satiety would make biological sense as a means of conserving stored energy. Deleting OXTRs specifically in adipocytes should yield further insight into this biology.

There is the unlikely possibility that OXT interacts with a vasopressin receptor, Avpr1a, on adipocytes. OXT does not appear to interact with Avpr1a on the osteoblasts (29). We also confirmed the existence of the OXTR on adipocytes not only by Western blot and immunohistochemistry analyses, but also by Sanger sequencing.

Finally, OXT triggered the expression of the steroidogenic enzyme 17β-hydroxysteroid dehydrogenase, which converts estrone to estradiol, in adipocytes. The physiological significance of the control of steroidogenesis by OXT in fat cells is currently unclear. Speculatively, however, high OXT levels in pregnancy may stimulate estrogen production from WAT to compensate for pregnancy-associated lowering of estrogen (19). Moreover, OXT dramatically stimulates the expression of *Serpine1*, the gene encoding PAI1. This phenomenon may contribute to the prothrombotic state in pregnancy when OXT levels are high. The action of exogenous OXT used to prevent excessive postpartum bleeding may also arise from the stimulation of PAI1 expression, as opposed solely to inducing vasoconstriction.

Overall, our study unmasks the biology of OXT, a primitive nonapeptide dating almost 100 million y (18), to encompass not only procreation, but also vital bodily functions, such as the regulation of bone mass, body composition and metabolism, and perhaps even thrombosis. The common physiological denominator, where all such actions seem to converge, are the conditions of physiological stress under which OXT levels are high, notably pregnancy and lactation. With that said, the use of the OXT signaling axis shows promise for the future development of therapeutics for osteoporosis and obesity, among other medical conditions.

Materials and Methods

Mouse experiments were performed in accordance with protocols approved by the Institutional Animal Care and Use Committees at Icahn Medical School at Mount Sinai. The generation of *Oxt*$^{-/-}$, *Oxtr*$^{-/-}$, *Acp5Cre*:*Oxtr*$^{fl/fl}$, and *Col2.3Cre*:*Oxtr*$^{fl/fl}$ mice has been reported previously (1, 5, 17, 30). Ovariectomy was performed as described previously (17). We used a small animal bone densitometer (Lunar Piximus; GE Healthcare) (31) to measure whole-body (cranium excluded), spine (L4 to L6), and femur and tibiae areal BMD, as described previously (17). High-resolution μCT scanning (μCT50; Scanco) was performed to measure microstructural parameters at the metaphyseal region of femur and/or lumbar vertebrae (L5-6), as described previously (15). In brief, the dissected bones were cleaned, fixed in 10% formalin, transferred to 75% (vol/vol) ethanol, loaded into 10-mm-diameter scanning tubes, and imaged, followed by reconstruction and 3D quantitative analyses of the images using the Scanco software. For histomorphometry, mice were injected with xylenol orange (90 mg/kg, i.p.) and calcein (15 mg/kg, i.p.) at 7 d and 2 d before sacrifice. Femurs were dissected, processed, and analyzed for bone formation parameters, as described previously (32). Primary cultures of bone marrow-derived stromal cells (14) were incubated in differentiation media for 7 or 21 d according to protocol (33) to count alkaline phosphatase-positive colony-forming unit fibroblastoids (CFU-F) and von Kossa stain-labeled mineralizing CFU-OB colonies, respectively.

Total RNA (1 μg) was reverse-transcribed using SuperScript II Reverse Transcriptase (Invitrogen). Gene expression was detected by qPCR using SYBR Select Master Mix (Life Technologies) on an Applied Biosystems ABI Prism 7900HT real-time thermocycler. Mouse *Gapdh*, *Actb*, *Tuba1b*, and *Rps11* genes were used for normalization. Primer sequences were as follows: Oxtr_F, 5′-TCATCGTGTGCTGGACGCCTTT-3′; Oxtr_R, 5′-GCCCGTGAAGAGCATGTAGATC-3′; Serpine1_F, 5′- CCTCTTCCACAAGTCTGATGGC-3′; Serpine1_R, 5′-GCAGTTCCACAACGTCATACTCG-3′;, Hsd17b12_F, 5′-ATGGTAGAAAGATCTAAAGGGG-3′; Hsd17b12_R, 5′-GAGAGAAGAAATCTACAAAGGC-3′; Irs1_F, 5′-GATCGTCAATAGCGTAACTG-3′; Irs1_R, 5′-ATCGTACCATCTACT-3′; Pparg_F, 5′-GTGCCAGTTTCGATCCGTAGA-3′; Pparg_R, 5′-GGCCAGCATCGTGTAGATGA-3′; Adipoq_F, 5′-GCACTGGCAAGTTCTACTGCAA-3′; Adipoq_R, 5′-GTAGGTGAAGAGAACGGCCTTGT-3′; Cebpa_F, 5′-GCAAAGCCAAGAAGTCGGTGGA-3′; Cebpa_R, 5′-CCTTCTGTTGCGTCTCCACGTT-3′; Insr_F, 5′-AAGACCTTGGTTACCTTCTC-3′; Insr_R, 5′-AAGACCTTGGTTACCTTCTC-3′; Fabp4_F, 5′-GTAAATGGGGATTTGGTCAC-3′; Fabp4_R, 5′-TATGATGCTCTTCACCTTCC-3′; Cox7a1_F, 5′-AGAAAACCGTGTGGCAGAGA-3′; Cox7a1_R, 5′-CAGCGTCATGGTCAGTCTGT-3′; Cox8b_F, 5′-GCGAAGTTCACAGTGGTTCC-3′; Cox8b_R, 5′-GAACCATGAAGCCAACGACT-3′; Cebpb_F, 5′-ATCACTTAAAGATGTTCCTGC-3′; Cebpb_R, 5′-ATCACTTAAAGATGTTCCTGC-3′; Retn_F, 5′-CCTCCTTTTCCTTTTCTTCC-3′; Retn_R, 5′-CATTTGGAAACAGGGAGTTG-3′; Cidea_F, 5′-TGGTGGACACAGAGGAGTTC-3′; Cidea_R, 5′-AGCCTGTATAGGTCGAAGGTG-3′; Actb_F, 5′-CATTGCTGACAGGATGCAGAAGG-3′; Actb_R, 5′-TGCTGGAAGGTGGACAGTGAGG-3′; Gapdh_F, 5′-CATCACTGCCACCCAGAAGACTG-3′; Gapdh_R, 5′-ATGCCAGTGAGCTTCCCGTTCAG-3′; Rps11_F, 5′-GCAGAGGACCATTGTCATCCGC-3′; Rps11_R, 5′-CTCCAACTGTGACAATGTCTCCG-3′; Tuba1a_F, 5′-GGCAGTGTTCGTAGACCTGGAA-3′; and Tuba1a_R, 5′-CTCCTTGCCAATGGTGTAGTGG-3′.

For protein expression studies, immunohistochemistry was performed on paraffin sections of various tissues using anti-OXTR (Abcam; ab181077) and anti-rabbit IgG HRP conjugate (Abcam; ab6721) as primary and secondary antibodies, respectively. Images were captured on an EVOS M5000 Cell Imaging System. Western blot analysis was performed using the same antibodies.

Data Availability. Our complete dataset is available at https://osf.io/ws98e/?view_only=8d17370ec6f74d88a909ed02f1c12321 (34).

ACKNOWLEDGMENTS. We thank Jay Cao, PhD for his assistance with the μCT analyses. M.Z. is supported by NIH Grants R01 AG40132, R01 AR67066, R01 DK113627, and U19 AG60917. M.I.N. is supported by the Maria I. New Children's Hormone Research Foundation. A.Z. is supported by the Italian Space Agency.

1. K. Nishimori *et al.*, Oxytocin is required for nursing but is not essential for parturition or reproductive behavior. *Proc. Natl. Acad. Sci. U.S.A.* **93**, 11699–11704 (1996).
2. Y. Takayanagi *et al.*, Pervasive social deficits, but normal parturition, in oxytocin receptor-deficient mice. *Proc. Natl. Acad. Sci. U.S.A.* **102**, 16096–16101 (2005).
3. S. Colucci, G. Colaianni, G. Mori, M. Grano, A. Zallone, Human osteoclasts express oxytocin receptor. *Biochem. Biophys. Res. Commun.* **297**, 442–445 (2002).
4. C. Elabd *et al.*, Oxytocin controls differentiation of human mesenchymal stem cells and reverses osteoporosis. *Stem Cells* **26**, 2399–2407 (2008).
5. R. Tamma *et al.*, Oxytocin is an anabolic bone hormone. *Proc. Natl. Acad. Sci. U.S.A.* **106**, 7149–7154 (2009).
6. I. MacIntyre *et al.*, Osteoclastic inhibition: An action of nitric oxide not mediated by cyclic GMP. *Proc. Natl. Acad. Sci. U.S.A.* **88**, 2936–2940 (1991).
7. N. Deblon *et al.*, Mechanisms of the anti-obesity effects of oxytocin in diet-induced obese rats. *PLoS One* **6**, e25565 (2011).
8. J. L. Holder, Jr, N. F. Butte, A. R. Zinn, Profound obesity associated with a balanced translocation that disrupts the SIM1 gene. *Hum. Mol. Genet.* **9**, 101–108 (2000).
9. D. F. Swaab, J. S. Purba, M. A. Hofman, Alterations in the hypothalamic paraventricular nucleus and its oxytocin neurons (putative satiety cells) in Prader-Willi syndrome: A study of five cases. *J. Clin. Endocrinol. Metab.* **80**, 573–579 (1995).
10. Y. Takayanagi *et al.*, Oxytocin receptor-deficient mice developed late-onset obesity. *Neuroreport* **19**, 951–955 (2008).
11. Y. Maejima *et al.*, Peripheral oxytocin treatment ameliorates obesity by reducing food intake and visceral fat mass. *Aging (Albany N.Y.)* **3**, 1169–1177 (2011).
12. G. J. Morton *et al.*, Peripheral oxytocin suppresses food intake and causes weight loss in diet-induced obese rats. *Am. J. Physiol. Endocrinol. Metab.* **302**, E134–E144 (2012).
13. X. S. Liu, G. Bevill, T. M. Keaveny, P. Sajda, X. E. Guo, Micromechanical analyses of vertebral trabecular bone based on individual trabeculae segmentation of plates and rods. *J. Biomech.* **42**, 249–256 (2009).

14. L. Sun *et al*., FSH directly regulates bone mass. *Cell* **125**, 247–260 (2006).
15. L. L. Zhu *et al*., Blocking antibody to the β-subunit of FSH prevents bone loss by inhibiting bone resorption and stimulating bone synthesis. *Proc. Natl. Acad. Sci. U.S.A.* **109**, 14574–14579 (2012).
16. S. Khosla, L. J. Melton, 3rd, B. L. Riggs, The unitary model for estrogen deficiency and the pathogenesis of osteoporosis: Is a revision needed? *J. Bone Miner. Res.* **26**, 441–451 (2011).
17. G. Colaianni *et al*., Bone marrow oxytocin mediates the anabolic action of estrogen on the skeleton. *J. Biol. Chem.* **287**, 29159–29167 (2012).
18. J. J. Wysolmerski, The evolutionary origins of maternal calcium and bone metabolism during lactation. *J. Mammary Gland Biol. Neoplasia* **7**, 267–276 (2002).
19. L. Ardeshirpour, S. Brian, P. Dann, J. VanHouten, J. Wysolmerski, Increased PTHrP and decreased estrogens alter bone turnover but do not reproduce the full effects of lactation on the skeleton. *Endocrinology* **151**, 5591–5601 (2010).
20. X. S. Liu, L. Ardeshirpour, J. N. VanHouten, E. Shane, J. J. Wysolmerski, Site-specific changes in bone microarchitecture, mineralization, and stiffness during lactation and after weaning in mice. *J. Bone Miner. Res.* **27**, 865–875 (2012).
21. J. N. VanHouten *et al*., Mammary-specific deletion of parathyroid hormone-related protein preserves bone mass during lactation. *J. Clin. Invest.* **112**, 1429–1436 (2003).
22. P. Liu *et al*., Blocking FSH induces thermogenic adipose tissue and reduces body fat. *Nature* **546**, 107–112 (2017).
23. A. Di Benedetto *et al*., Osteoblast regulation via ligand-activated nuclear trafficking of the oxytocin receptor. *Proc. Natl. Acad. Sci. U.S.A.* **111**, 16502–16507 (2014).
24. X. Liu *et al*., Oxytocin deficiency impairs maternal skeletal remodeling. *Biochem. Biophys. Res. Commun.* **388**, 161–166 (2009).
25. M. Zaidi, Skeletal remodeling in health and disease. *Nat. Med.* **13**, 791–801 (2007).
26. M. Zaidi *et al*., Actions of pituitary hormones beyond traditional targets. *J. Endocrinol.* **237**, R83–R98 (2018).
27. Y. Ji *et al*., Epitope-specific monoclonal antibodies to FSHβ increase bone mass. *Proc. Natl. Acad. Sci. U.S.A.* **115**, 2192–2197 (2018).
28. N. Sabatier, G. Leng, J. Menzies, Oxytocin, feeding, and satiety. *Front. Endocrinol. (Lausanne)* **4**, 35 (2013).
29. L. Sun *et al*., Functions of vasopressin and oxytocin in bone mass regulation. *Proc. Natl. Acad. Sci. U.S.A.* **113**, 164–169 (2016).
30. H. J. Lee, H. K. Caldwell, A. H. Macbeth, S. G. Tolu, W. S. Young, 3rd, A conditional knockout mouse line of the oxytocin receptor. *Endocrinology* **149**, 3256–3263 (2008).
31. L. L. Zhu *et al*., Vitamin C prevents hypogonadal bone loss. *PLoS One* **7**, e47058 (2012).
32. R. Baliram *et al*., Thyroid and bone: Macrophage-derived TSH-β splice variant increases murine osteoblastogenesis. *Endocrinology* **154**, 4919–4926 (2013).
33. G. Colaianni *et al*., Regulated production of the pituitary hormone oxytocin from murine and human osteoblasts. *Biochem. Biophys. Res. Commun.* **411**, 512–515 (2011).
34. T. Yuen, Oxytocin and body composition. Open Science Framework. https://osf.io/ws98e/?view_only=8d17370ec6f74d88a909ed02f1c12321. Deposited 25 November 2019.